Human Brain Microvascular Endothelial Cells Resist Elongation Due to Shear Stress

Adam Reinitz,[#] Jackson DeStefano,[#] Mao Ye, Andrew D. Wong, and Peter C. Searson[*]

[1]Department of Materials Science and Engineering, Johns Hopkins University, 3400 North Charles Street, Baltimore, MD 21218, USA

[2]Institute for Nanobiotechnology Johns Hopkins University, 3400 North Charles Street, Baltimore, MD 21218, USA

[#]contributed equally

Supplementary Video 1. A confluent monolayer of HBMECs under a shear stress of 16 dynes cm^{-2} for 36 hours after 6 hours pre-conditioning. Area is 1.5mmx 1.2mm.

Supplementary Video 2.A confluent monolayer of HUVECs under a shear stress of 16 dynes cm^{-2} for 72 hours after 6 hours pre-conditioning. Area is 1.5 mmx 1.2 mm.

Supplementary Information

1. Verification of flow profile

2. Analysis of time lapse videos

3. Verification of morphological parameters from time-lapse videos

4. Particle Image Velocimetry

5. Influence of growth factors on cell morphology and cell speed

6. Analysis of f-actin filament orientation

7. Macro for morphological analysis of time-lapse videos

1.Verification of flow profile

To verify the flow profile in the microfluidic channels, fluorescent beads (Fluospheres, 2.0 μm, red, Invitrogen) were injected into the flow system. After the beads had dispersed throughout the system a series of videos were taken. Videos were recorded in 50 μm increments, starting from the height of the cell monolayer and continuing to the top of the channel. Each video consisted of ~140 frames which covered a time of about 9 seconds, or the period of our peristaltic pump. Each frame is taken at either 4ms or 6ms exposure time and consists of numerous lines, representing flowing beads, some in focus and some out of focus(Figure S1). In order to calculate the velocity of the beads, each line that is in focus is traced. This gives the length in pixels of the lines in focus as a function of time. Since the scale of the image is 0.64 microns/pixel and the exposure time for each image is known, a velocity can be extracted from the length of these lines. By tracing frames along the entire period of the peristaltic pump for each height we were then able to compose a velocity as a function of time graph (Figure S2a), showing how the velocity of the flow changes along the period of the pump. Once those numbers were obtained we can then take the min, max, and time average velocities at each height and show velocity as a function of height (Figure S2b), giving us the flow profile.
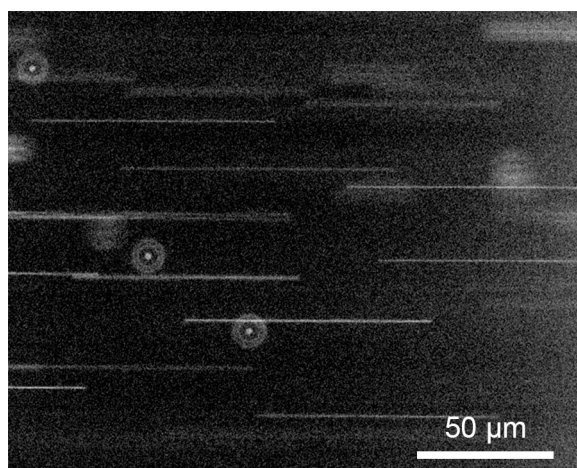

Figure S1. Sample image of fluorescent beads flowing through the 4 dyne cm^{-2} channel
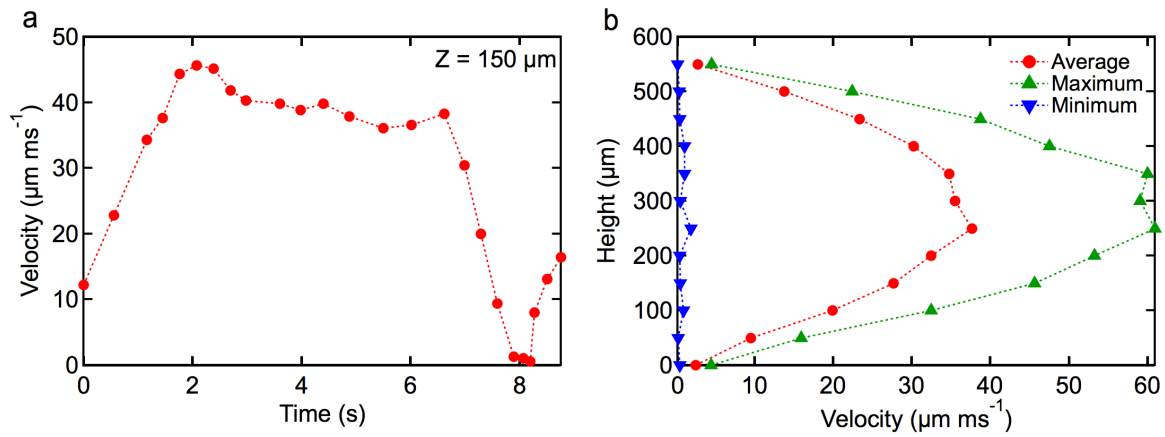
Figure S2. (a) Plot of velocity versus time at a height of 150 μm above the cell monolayer in the 4 dyne cm^{-2} channel. This plot demonstrates the peristaltic flow with a period of ~9s. (b) Plot of channel height versus velocity, with the expected parabolic shape. The curves shown represent the maximum, minimum, and time average velocity at each height.

2. Analysis of time lapse videos

The first step to analyze the time lapse video is to select the frames that are going to be analyzed and export them as a series of .tif images. We select an image every six hours throughout the run, and the images are exported in a mono-image format. To analyze the selected frames an ImageJ macro is used that traces each individual cell and outputs relevant statistics. The macro is run on each frame, generating data that describes how the monolayer changes as a function of time and shear stress. All the data is then compiled in an excel spreadsheet in order to visualize the trends.
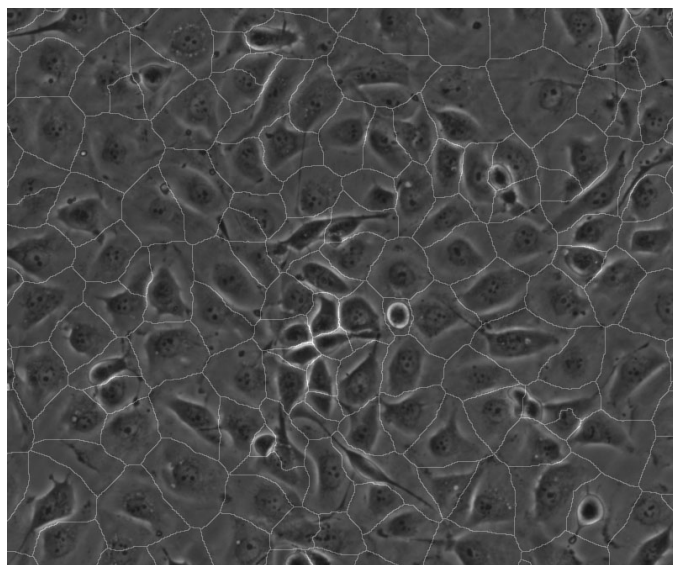
Figure S3. Overlay of the skeleton output from the cell tracing macro over the original phase-contrast image.

3. Verification of morphological parameters from time-lapse videos

To verify that our ImageJ macro accurately traces cell-cell boundaries, immunofluorescence images of ZO-1 borders were hand traced and compared to the results from the macro. The results from this comparison (Table S1) indicate that the macro is sufficiently accurate in tracing, with a maximum error of 7.3% in the 12 dyne cm^{-2} area parameter and an average error across all parameters of 4.7%. By increasing the number of cells hand traced this error may be reduced, but

this sample size was sufficient for the verification purposes. A second, more qualitative method was also employed to further verify the computer traces. To be specific, when the ImageJ macro runs a skeleton is saved, which is a mask of all the cells traced. Using Adobe Photoshop, this skeleton is layered on top of the original image that was traced. By reducing the opacity of the skeleton, it is possible to see the mask of the traced cells over the image (Figure S3) of the cell monolayer and, therefore, visually confirm that the trace is accurate.

shear stress	8 dyne cm^{-2}		12 dyne cm^{-2}	
method	IHC	macro	IHC	macro
N	494	4589	488	863
Area	1160 ± 27	1090 ± 8	1270 ± 7	1370 ± 25
Orientation	19.4 ± 0.5	18.5 ± 0.2	19.4 ± 0.5	19.4 ± 0.4
IAR	0.25 ± 0.003	0.26 ± 0.001	0.25 ± 0.003	0.27 ± 0.002

Table S1. Comparison of morphological parameters for HBMECs obtained from our automated ImageJ macro (macro) and from manual tracing of ZO-1 cell borders in fluorescence images (IHC). HBMECs were exposed to a shear stress of 8 dyne cm^{-2} or 12 dyne cm^{-2} for 36 h. Parameters are expressed ± SE.
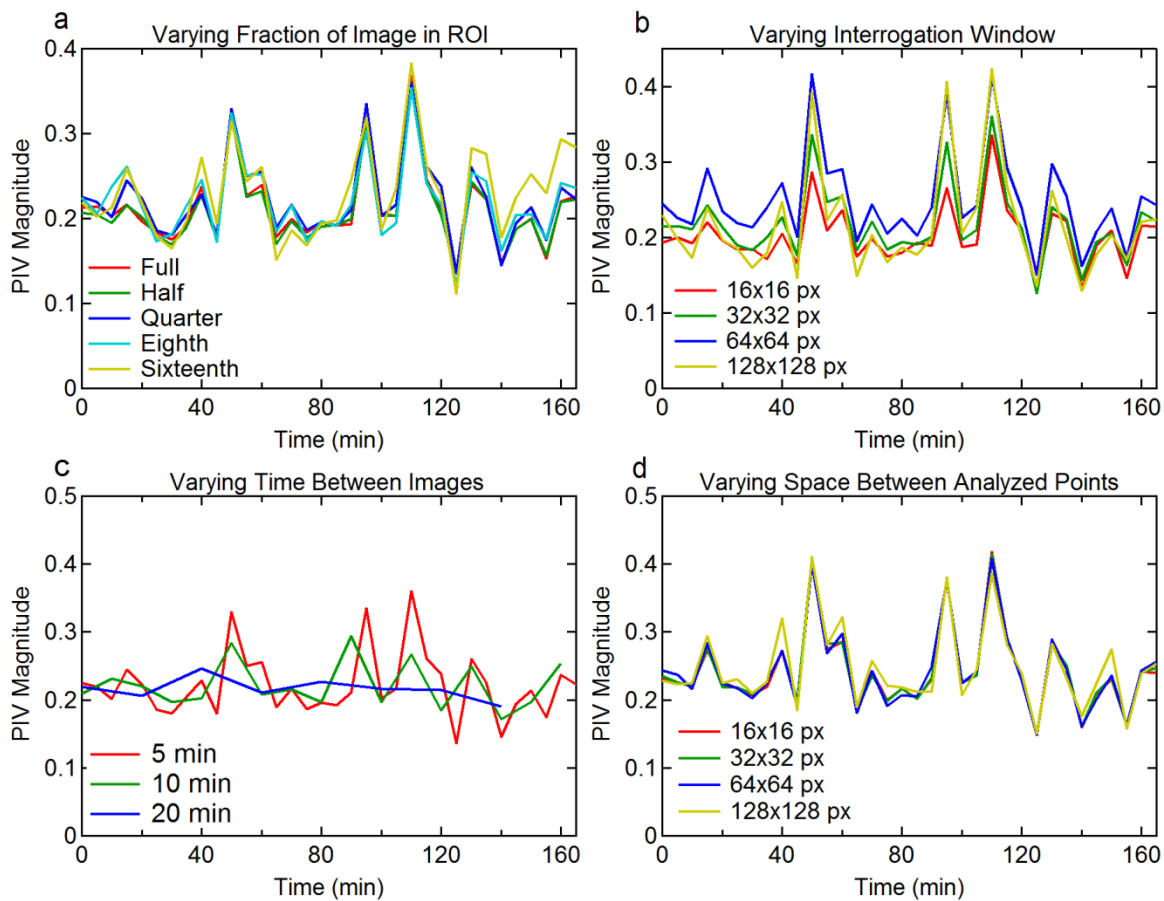
4. Particle Image Velocimetry

The OpenPIV application was used to analyze the motility of cell monolayers exposed to shear stress. This application has several parameters that can be selected to optimize either the resolution or run time. In order to validate the robustness of the application, each of these parameters was adjusted to determine its influence on the output data. Data are presented here on the effect of the interrogation window, the spacing/overlap, the size of the region of interest (ROI), and time difference between successive images. The S/N parameters were tested but did not alter the output data. The scale parameter does not affect the analysis and, therefore, was also omitted from the validation. The results reported here are unfiltered, meaning points that were outliers were not filtered out, and therefore the outlier filter is not important for consideration here. The jump parameter allows comparison of each image to an image further along in the image sequence, smoothing data, while preventing analysis of several final time points. In order to analyze the entire experiment, the jump parameter was left at 1 for the motility analysis.
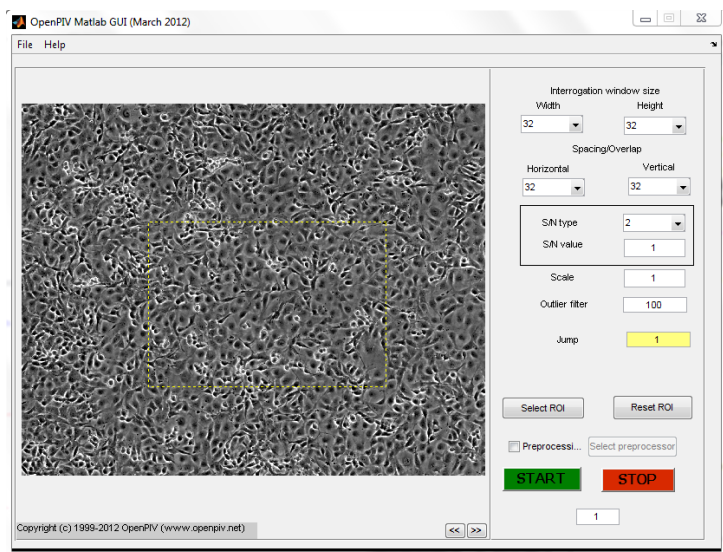
Figure S3. Screenshot of the OpenPIV GUI, with analyzing parameters listed (*right*) and a sample ROI outlined by the yellow box

The results from the validation experiments (Figure S4) indicate that changing any of these parameters does no significantly change the observed motility. Reducing the size of the ROI (Figure S4a) slightly increases the noise in the data, but the output data continues to fluctuate around a value of 0.2. Since increasing the ROI significantly slows the program down, the motility analysis was performed with an ROI containing a quarter of the full image. Increasing the size of the interrogation window (Figure S4b) increases the apparent noise in the data. Since the interrogation window determines the area within which the program will look for the next location of each point, it is likely that with larger interrogation windows large, outlier jumps will be included in the data. Increasing the interrogation slows the program even more significantly than the high ROI, and, therefore, a 32x32 pixel interrogation window was chosen for the motility analysis. Varying the time between images (Figure S4c) causes a smoothing of the data, but does significantly change the average PIV recorded. For the full experiments, time-lapse images are captured every 20 min and, based on these results, this imaging frequency is sufficient to capture the motility trends as a function of time. Reducing the space between analyzed points (Figure S4d) increases the number of data points collected for each image. This does not appear to significantly alter the output data and, for spacing below 32x32 pixels, reduced spacing causes the program to run extremely slow. For this reason, the spacing/overlap was set to 32x32 pixels. None of the parameters significantly affected the output and, therefore, the settings were chosen to maximize the speed of the program without sacrificing the resolution of the resulting data.

a — Varying Fraction of Image in ROI

b — Varying Interrogation Window

c — Varying Time Between Images

d — Varying Space Between Analyzed Points

Figure S4. Plots of motility data from adjusting (a) the ROI, (b) the interrogation window, (c) the time between images, and (d) the spacing/overlap between analyzed points.

Comparison of PIV to analysis of individual cells

To determine how well the PIV measurements represent individual cell speed, we traced individual cells
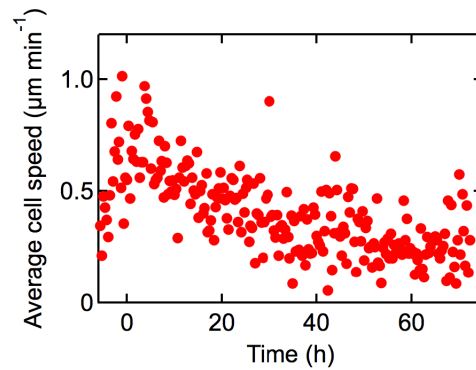
Figure S5. Average cell speed for HUVEC cells in endothelial basal media under 4 dyne cm^{-2} shear stress for 72 h (N = 4) determined by individual cell tracking. To track an individual cell, the x,y location of the cell nucleus was identified in each frame and the cell speed calculated from the displacement. The time dependence of the cell speed is qualitatively the same as the PIV measurement (Figure 5b), however, the magnitude of the cell speed is about two times higher than for the PIV measurements.

## 5. Influence of growth factors on cell morphology and cell speed
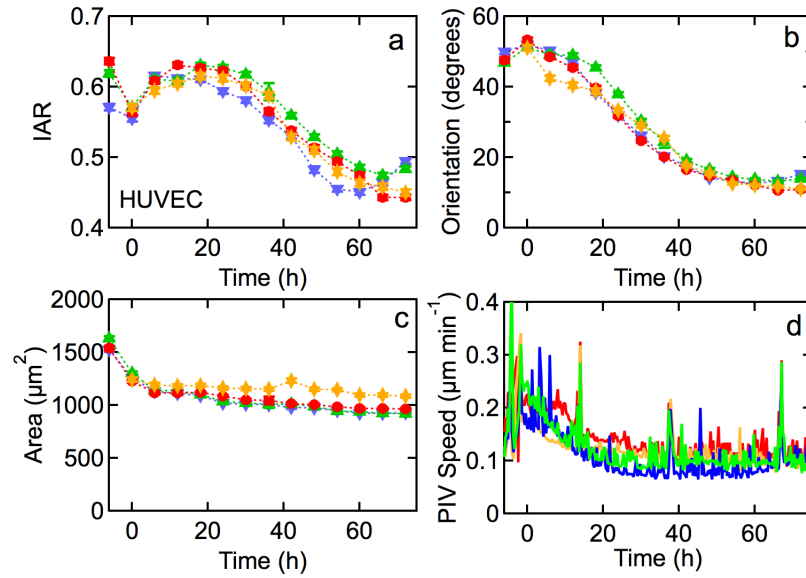
Figure S6. Morphology and speed of HUVECs in confluent monolayers exposed to a shear stress of 4, 8, 12, and 16 dyne cm^{-2} in basal media containing growth factors. (a) Inverse aspect ratio (IAR), (b) average angular orientation (θ), (c) average cell area (A), and (d) average cell speed. The average speed was determined using the PIV algorithm (see Materials and Methods) in basal media with growth factors. Data were obtained from analysis of images from time-lapse videos at 20 minute intervals. These results suggest that the presence of growth factors does not significantly influence cell morphology and cell speed.

6. Analysis of f-actin filament orientation

Fast Fourier transforms of 884 μm x 884 μm images (900 pixels x 900 pixels) were obtained using the FFT2 routine in MATLAB. The reciprocal space intensity distributions for HBMECs and HUVECs at 8, 12, and 16 dyne cm^{-2} are shown in Figure S7. The radial intensity distributions are obtained by integrating the intensity in 10° increments (Figure S8).
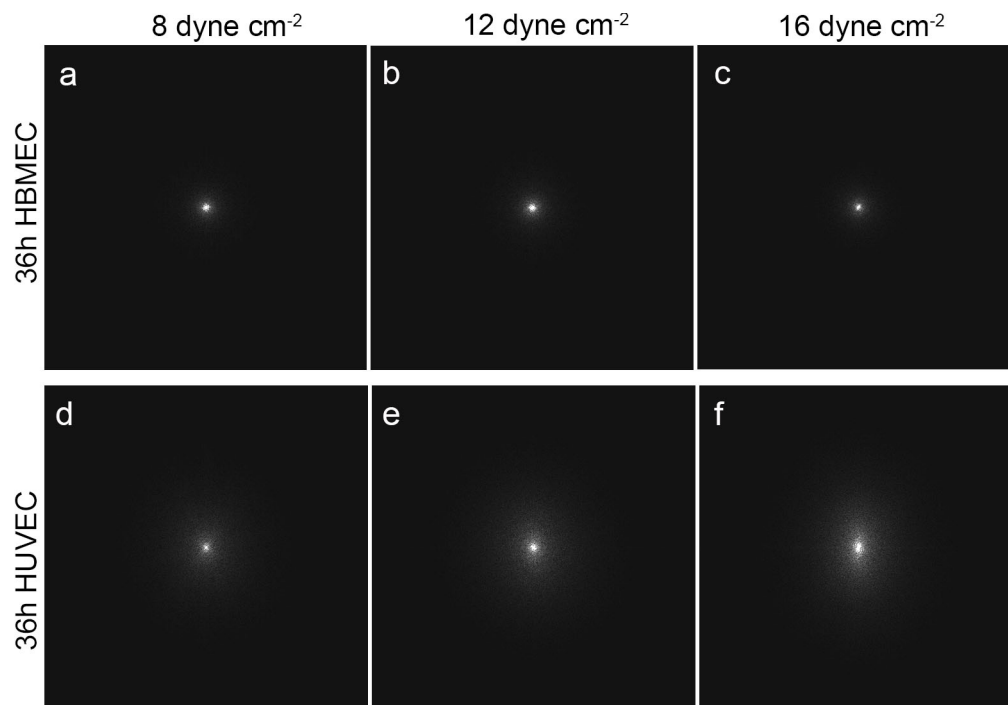
Figure S7. Fast Fourier Transform images showing the distribution of fluorescence intensity in reciprocal space, with the zero-frequency pixel in the center. Fourier transforms were performed on 884 μm x 884 μm images (900 pixels x 900 pixels). Orientation data for each condition are calculated by averaging the intensity distribution of three transform images obtained from different locations in the channel. Brightness and contrast adjustments were made uniformly to each of these image.
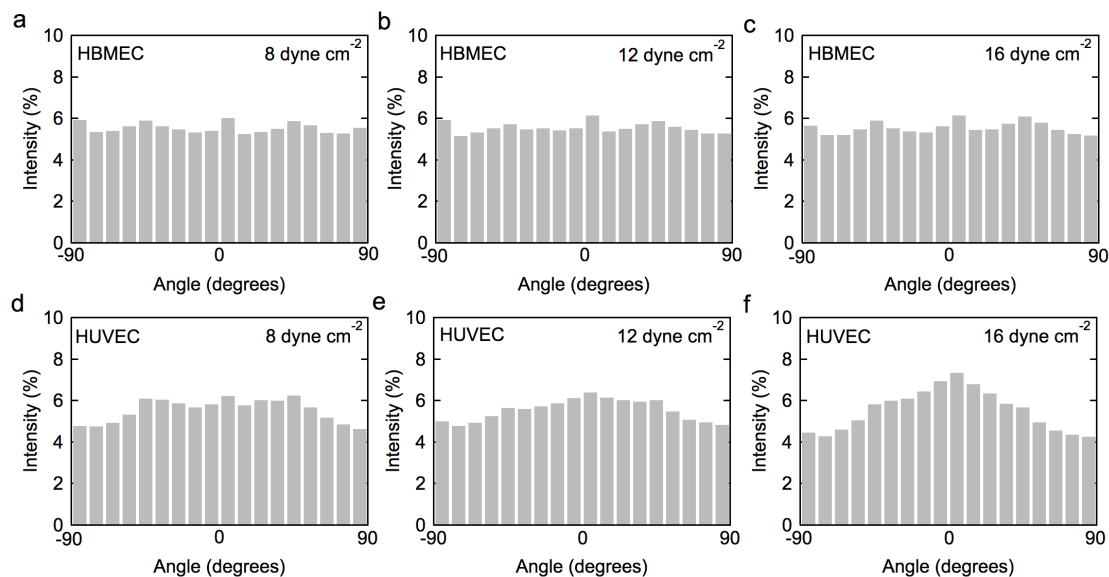
Figure S8. Radial intensity distributions of actin filament alignment from -90° to 90°. Each graph corresponds to the associated transform image in Figure S7. The parallel indices were obtained from the intensity in the range $0 \pm 10°$ and the perpendicular indices were obtained from intensities in the range $90 \pm 10°$ bins.

To verify the robustness of the F-actin quantification program, validation experiments were conducted to confirm the consistency and tolerances of the protocol. Validation experiments were designed to determine how varying the image size, the image resolution, and the region imaged would affect the results obtained. Fluorescence images of HUVECs exposed to 16 dyne cm^{-2} for 72h and stained for F-actin were chosen for the validation because these cells showed the most significant variation from a random distribution and, therefore, would be expected to show more discernible changes when varying these parameters.

Results from varying the image size (Figure S9) indicate that reducing the image size increases the variability of measurements between images but does not significantly alter the average value, with measured values for actin parallel to flow of 21.7% ±.2% when analyzing the complete image and 20.7% ± 1.6% when analyzing 1/64 of the image. Similarly, the actin perpendicular to flow was recorded as 6.36% ± .06% when analyzing the full image and 6.77% ±

.09% when analyzing 1/64 of the image. The data reported in this paper is the average analysis of 3 full size images, each containing more than 500 cells.
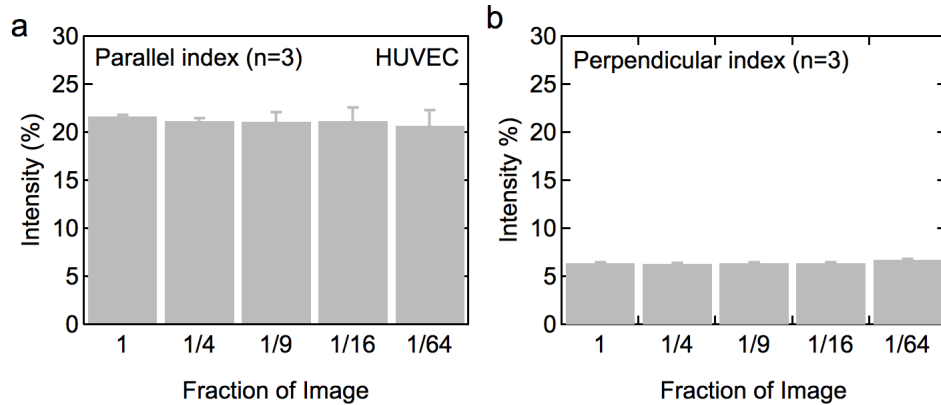
Figure S9. Influence of image size on fraction of oriented filaments. A 900 x 900 pixel (884 μm x 884 μm) image was used for analysis. (a) Parallel and (b) perpendicular index for different fractions of the full image analyzed.

Results from decreasing the image resolution (Figure S10) indicate that reducing the resolution by up to a factor of 8 does not significantly alter the measured values with values for percent actin parallel to flow of 21.8 at full resolution, 21.4 at 1/3 resolution, and 19.8 at 1/8 the resolution. Similarly, the percent actin perpendicular to flow was measured as 6.3 at full resolution, 6.2 at 1/3 resolution and 6.7 at 1/8 resolution. This data was based on a single image containing more than 500 cells.

Images were taken from three separate regions within the channel to confirm consistency between images. The measured values for actin parallel at these three locations were 21.8%, 21.2%, and 22.0%. The measured values for actin perpendicular at these three locations were 6.3%, 6.5%, and 6.2%. These results indicate that the program measured actin fibers to be consistently non-random throughout the channel.
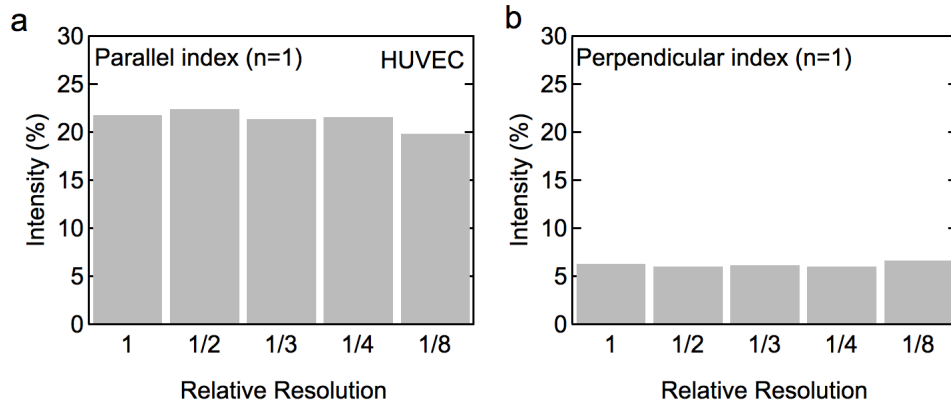
Figure S10. Plots of the percent of actin parallel (*left*) and perpendicular (*right*) to the direction flow versus the relative resolution, as compared to the uncompressed (full) image.

7. Macro for morphological analysis of time-lapse videos

To quantify the morphological parameters of HBMEC and HUVEC monolayers we use a custom imageJ macro, CellTracer. CellTracer traces individual cells in a phase contrast image of a confluent monolayer and outputs the area, orientation angle, and inverse aspect ratio for each cell traced. The code for the macro is provided below:

```
fpath = "/C:/imageStack/"; //Define File Path, specifies the location of the sequence of .tif
images
i=3; //Naming the number of the image in the set, defines the xy-position, to be changed to
chage which image to analyze
thresh=100;//lower bound value for setThreshold()
run("Clear Results"); //Empty the results table

//Image Processing
    run("Enhance Contrast", "saturated=90"); //Increase contrast
    for (j=0;j<10;j++){
            run("Smooth"); //Smooths edges between the cell body and border
    }
    setAutoThreshold("Default dark");  //Applies threshold to set any not black regions as
background
    setThreshold(thresh, 255); //sets threshold, vary first number to optimize image
analysis, may be necessary to comment out
    run("Convert to Mask"); // Converts the thresholded image to a binary mask
    run("Convert to Mask"); // Inverts black and white on the mask
    run("Fill Holes");

    run("Analyze Particles...", "size=300-Infinity circularity=0.00-1.00 show=Masks display");
//Removes particles smaller than this lower bound
    run("Find Maxima...", "noise=10 output=[Segmented Particles] light"); //Applies
algorithm to expand cells to fill the image area
    run("Clear Results"); //Removes results from analyze particles
    run("Analyze Particles...", "size=700-16000 circularity=0.00-1.00 show=Masks display
add"); //Analyzes the expanded cells

//Preparing location to save the traced monolayer
    File.makeDirectory(fpath + "skeleton"); //Creates folder to save monolayer trace
    fsave = fpath + "skeleton/" + "seg" + iname; //Create file for monolayer trace

//Save monolayer trace
    selectWindow("Mask of " + iname); close();
```

```
selectWindow(iname); close();
selectWindow("Mask of " + iname + " Segmented");
saveAs("Tiff",fsave); // Saving skeleton
close()
```

USER MANUAL

Image Acquisition & Export

(1) Take time-lapse images of a uniform monolayer of endothelial cells. We typically collect phase-contrast images on an inverted microscope (Nikon Instruments) with a 10x objective every 20 min using a 14-bit grayscale camera and automated image acquisition software (NIS Elements). Select frames for analysis.

(2) Export images as grayscale tif files to be analyzed using ImageJ (NIH, Bethesda, MD).

Image Analysis using ImageJ

(1) Open ImageJ (Figure 1).

(2) Import time-lapse images as an image stack: File>Import>Image Sequence...

(3) Open the ImageJ macro for editing: Plugins>Macros>edit...

(4) Optimize threshold variables.

    (a) 'thresh'

        • thresh is an integer value used in the "setThreshold" method. This variable should contain an 8-bit value, between 0 and 255. This value is optimized for one or more images to enhance the borders between cells when converting the images to binary. We manually check the resulting binary image for discrete borders and iteratively adjust the number for improvement; our values typically range from 60 to 150.

        • In Figure 2, three different traces are shown each having a different threshold value. At the optimal value, 110 in this case, all the cells are recognized and traced (Figure 2b). If the thresh is too high, 130 in this example, the macro recognizes particles that are not cells which causes errors in the trace (Figure 2a). Similarly if the threshold is too low the macro does not recognize all the cells leading to errors in the trace (Figure 2c).

(b) There is a saturated value for the "Enhance Contrast" at the beginning of the image processing block that can be changed but the best results are obtained at a value of 90.

(c) There is also a loop of smooth methods run after the "Enhance Contrast" method and the number of iterations can be change but the best results are obtained at a value of 10.

(d) For the analyze particles method there is an upper and lower bound particle size which determines which particles get expanded. The lower bound is set at 200 pixels. This number has some room to change if there are smaller cells, but by decreasing the lower bound there is an increased possibility of expanding a particle that is not a cell. The upper bound is set to infinity.

(e) There is also a second iteration of analyze particles that analyzes the traced cells to see if there are any errors. There is a size field that can be modified which tells the program which cells to exclude, if any, based on being either too small or too large to be a cell.

(5) Select relevant parameters (Area, Center of mass, Perimeter, Shape descriptors, etc.) to be measured: *Analyze -> Set Measurements* (Figure 3).

(6) Save and run macro (Ctrl + S, Ctrl + R) (Figure 4).

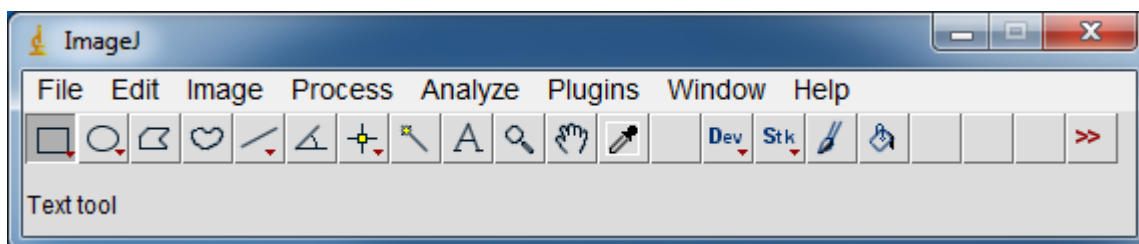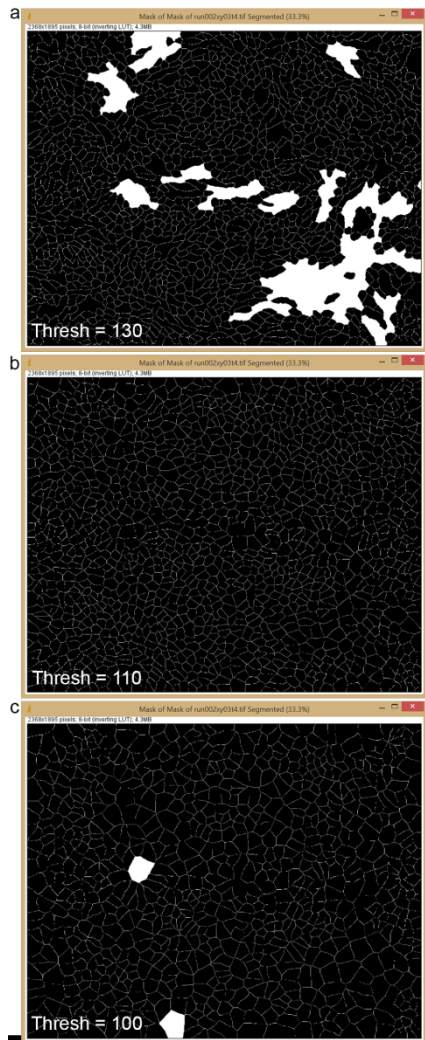(7) All relevant data is stored in the results table using Export/save data (Figure 5).
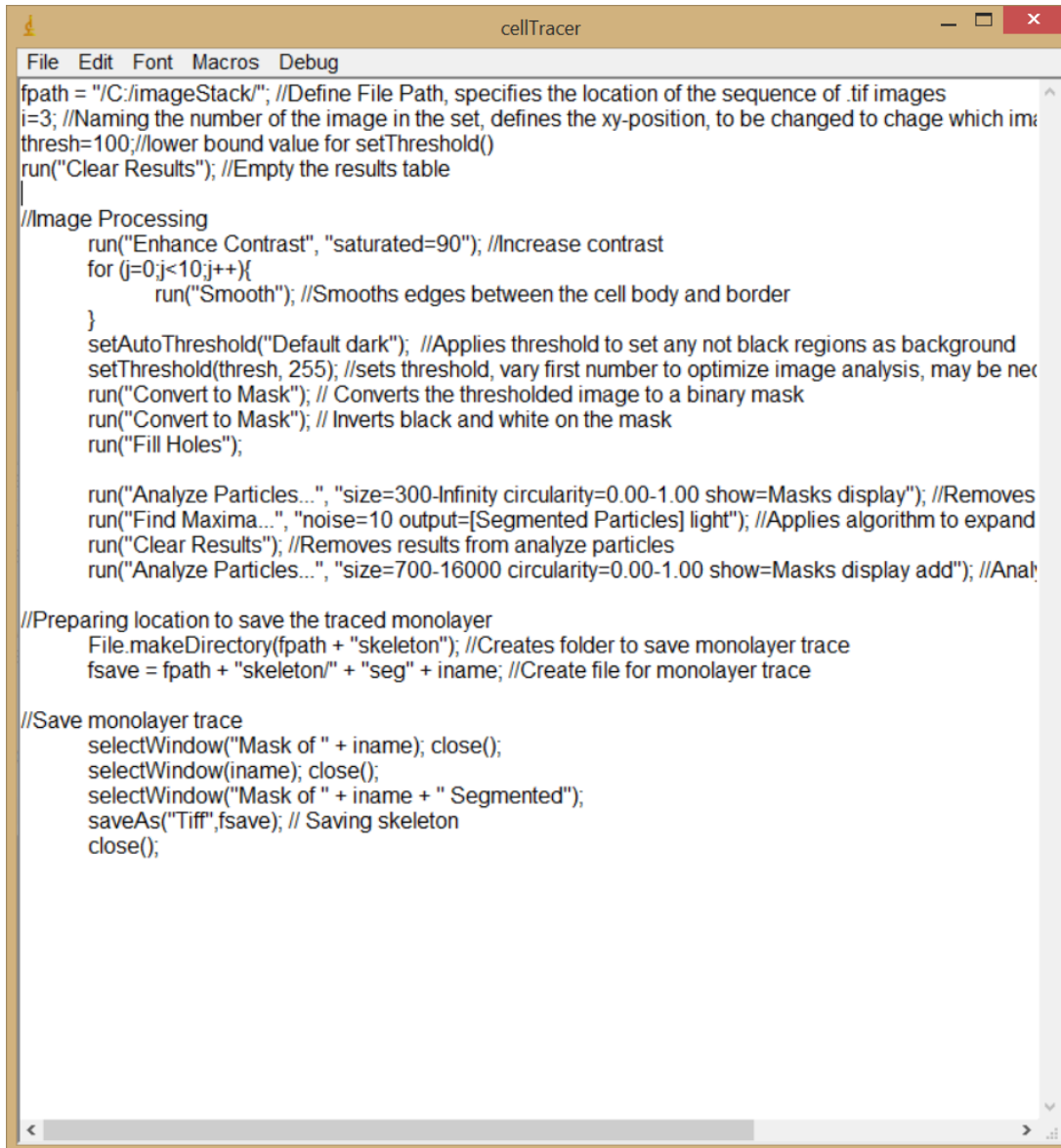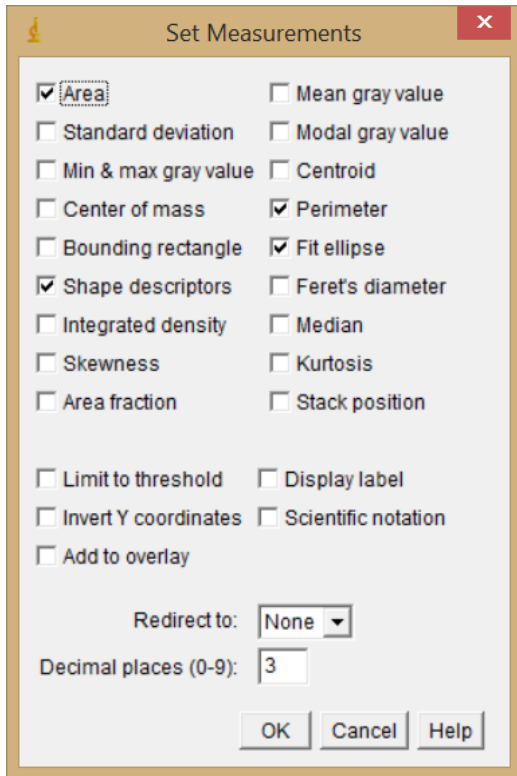

Figure 1

Figure 2

Figure 3

```
cellTracer                                              — □ ×

File  Edit  Font  Macros  Debug

fpath = "/C:/imageStack/"; //Define File Path, specifies the location of the sequence of .tif images
i=3; //Naming the number of the image in the set, defines the xy-position, to be changed to chage which ima
thresh=100;//lower bound value for setThreshold()
run("Clear Results"); //Empty the results table

//Image Processing
        run("Enhance Contrast", "saturated=90"); //Increase contrast
        for (j=0;j<10;j++){
                run("Smooth"); //Smooths edges between the cell body and border
        }
        setAutoThreshold("Default dark");  //Applies threshold to set any not black regions as background
        setThreshold(thresh, 255); //sets threshold, vary first number to optimize image analysis, may be nec
        run("Convert to Mask"); // Converts the thresholded image to a binary mask
        run("Convert to Mask"); // Inverts black and white on the mask
        run("Fill Holes");

        run("Analyze Particles...", "size=300-Infinity circularity=0.00-1.00 show=Masks display"); //Removes
        run("Find Maxima...", "noise=10 output=[Segmented Particles] light"); //Applies algorithm to expand
        run("Clear Results"); //Removes results from analyze particles
        run("Analyze Particles...", "size=700-16000 circularity=0.00-1.00 show=Masks display add"); //Analy

//Preparing location to save the traced monolayer
        File.makeDirectory(fpath + "skeleton"); //Creates folder to save monolayer trace
        fsave = fpath + "skeleton/" + "seg" + iname; //Create file for monolayer trace

//Save monolayer trace
        selectWindow("Mask of " + iname); close();
        selectWindow(iname); close();
        selectWindow("Mask of " + iname + " Segmented");
        saveAs("Tiff",fsave); // Saving skeleton
        close();
```

Figure 4

	Area	Perim.	Major	Minor	Angle	Circ.	AR	Round	Solidity
1135	5624	326.492	92.884	77.093	159.053	0.663	1.205	0.830	0.917
1136	6792	323.747	104.579	82.692	8.185	0.814	1.265	0.791	0.953
1137	3745	275.380	107.941	44.175	23.645	0.621	2.443	0.409	0.915
1138	4395	262.936	81.096	69.003	7.846	0.799	1.175	0.851	0.955
1139	2516	214.551	72.500	44.186	36.145	0.687	1.641	0.609	0.906
1140	9050	399.723	139.911	82.358	2.871	0.712	1.699	0.589	0.959
1141	3839	247.321	85.144	57.408	18.506	0.789	1.483	0.674	0.960
1142	5196	327.321	104.815	63.119	157.301	0.609	1.661	0.602	0.914
1143	8621	406.368	145.688	75.343	1.714	0.656	1.934	0.517	0.949
1144	3704	267.137	78.981	59.712	145.743	0.652	1.323	0.756	0.953
1145	9452	786.375	296.177	40.633	2.672	0.192	7.289	0.137	0.590
1146	3913	271.380	89.641	55.579	19.355	0.668	1.613	0.620	0.962
1147	4452	279.439	93.277	60.770	1.877	0.716	1.535	0.652	0.964
1148	5416	331.095	130.924	52.671	3.794	0.621	2.486	0.402	0.968
1149	1886	194.409	64.788	37.065	13.198	0.627	1.748	0.572	0.894
1150	3723	255.397	87.496	54.177	178.012	0.717	1.615	0.619	0.967
1151	3036	260.569	108.627	35.586	177.892	0.562	3.053	0.328	0.948

Figure 5